

## Monitoring Temporal Evolution of Silicate Species during Hydrolysis and Condensation of Silicates Using Mass Spectrometry

Stefan A. Pelster, Wolfgang Schrader, and Ferdi Schüth\*

Contribution from the Max-Planck-Institut für Kohlenforschung, Kaiser-Wilhelm-Platz 1, 45470 Mülheim, Germany

Received October 31, 2005; E-mail: schueth@mpi-muelheim.mpg.de.

**Abstract:** The first stages of solid-state formation from solution can be crucial in determining the properties of the resulting solids. We are trying to approach prenucleation reactions of silicates from an aqueous solution containing tetraalkylammoniumhydroxides (TAAOH) and tetraalkoxysilanes (TAOS) by analyzing hydrolysis and condensation using electrospray mass spectrometry (ESI MS). Time-resolved measurements were performed using different reactor systems to show the stepwise hydrolysis of the silanes and subsequent condensation of silicate monomers via oligomers to form larger units. We approached the precipitation point by varying the pH and the concentrations of the reactants. The results show the evolution of different silicate species occurring during condensation. No defined molecular entities were identified at pH values close to precipitation, which suggests that under the conditions used, solids are probably not formed from defined building blocks.

### Introduction

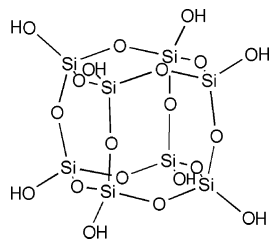
Solid-state formation from solution is one of the most important chemical reactions. In classical nucleation theory, it includes prenucleation, nucleation, and crystal growth, each of which is a topic of enduring interest in chemical sciences.<sup>1,2</sup> However, there is growing evidence that, in the formation of many complex solids, the sequence of events is rather more complex and that there possibly is not such a process as a single nucleation event, i.e., a maximum in the energy of the system caused by the balancing of the bulk and surface energy contributions with increasing particle size.<sup>3,4</sup> Instead, the formation of a solid from homogeneous solution may rather be considered as a series of chemical reaction steps, each one of which may have its own activation energy. The result of the solid-state formation process can be, for instance, a large single crystal or crystals in the nanometer size range for applications requiring large surface areas, such as catalysts. The early stages of particle formation, especially the nucleation step—if it occurs as a defined step—can have great relevance in controlling the microscopic properties as well as the macroscopic properties of the final solid. However, little is known about the nucleation and growth processes during the initial few hours of the crystallization for most systems, although some very detailed mechanisms for particle formation are proposed in the literature.<sup>5</sup> Because of the importance of the early stages of particle formation, it is highly desirable to learn more about the events

occurring within this time period on a molecular level. With this knowledge, it should eventually be possible to move away from a synthesis, which in the past often has been based on an empiric method of “trial and error”, and to rationally improve structural control in the synthesis of important materials such as zeolites.

The many uncertainties in the nucleation process arise from its brevity and from the small size scale, which prevent a prediction of when and where it will appear. Unfortunately, only very few experimental techniques are available to catch the nucleation spot and to analyze typical clusters of no more than a few hundred atoms, and no technique is able to capture the total nucleation mechanism completely on its own. One of the most powerful techniques revealing structural information about species in solution and nucleation processes is nuclear magnetic resonance (NMR) spectroscopy. Earliest experiments on the investigation of silicates using <sup>29</sup>Si NMR spectroscopy originate from Lippmaa and Engelhardt et al.<sup>6–10</sup> Further fundamental studies concerning condensed silicate species in alkoxide solutions as well as in solutions containing quaternary ammonium cations have been published by Knight et al. in a series of measurements using <sup>29</sup>Si NMR spectroscopy.<sup>11–14</sup> They

- (1) Mann, S.; Ozin, G. A. *Nature* **1996**, *382*, 313.
- (2) Kulmala, M.; Pirjola, L.; Mäkelä, J. M. *Nature* **2000**, *404*, 66.
- (3) Schüth, F. *Curr. Opin. Solid State Mater. Sci.* **2001**, *5*, 389.
- (4) Schüth, F.; Bussian, P.; Agren, P.; Schunk, S.; Linden, M. *Solid State Sci.* **2001**, *3*, 801.
- (5) Kirschhock, C. E. A.; Ravishankar, R.; Jacobs, P. A.; Martens, J. A. J. *Phys. Chem. B* **1999**, *103*, 11021.

- (6) Lippmaa, E. T.; Alla, M. A.; Pehk, T. J.; Engelhardt, G. *J. Am. Chem. Soc.* **1978**, *100*, 1929.
- (7) Hoebbel, D.; Garzo, G.; Engelhardt, G.; Ebert, R.; Lippmaa, E. T.; Alla, M. A. *Z. Anorg. Allg. Chem.* **1980**, *465*, 15.
- (8) Lippmaa, E. T.; Mägi, M.; Samoson, A.; Engelhardt, G.; Grimmer, A. R. *J. Am. Chem. Soc.* **1980**, *102*, 488.
- (9) Engelhardt, G.; Hoebbel, D. *Z. Chem.* **1983**, *23*, 33.
- (10) Hoebbel, D.; Garzo, G.; Engelhardt, G.; Vargha, A. *Z. Anorg. Allg. Chem.* **1982**, *494*, 31.
- (11) Knight, C. T. *J. Chem. Soc., Dalton Trans.* **1988**, 1457.
- (12) Harris, R. K.; Knight, C. T. *J. Mol. Struct.* **1982**, *78*, 273.
- (13) Harris, R. K.; Knight, C. T. *J. Chem. Soc., Faraday Trans. 2* **1983**, *79*, 1525.



**Figure 1.** Silicate species consisting of 8  $\text{HOSi}(\text{OSi})_3$  ( $\text{Q}^3$ ) silicon sites and exhibiting the geometry of a cubic octamer or double 4 ring (D4R) forms as the main product from silicate solutions containing tetraalkylammonium ions.<sup>11–14</sup>

identified a  $\text{Si}_8\text{O}_{20}\text{H}_8$  species, the cubic octamer, as the main product of the condensation reaction in solutions containing tetraalkylammonium ions and were also able to show the kinetics leading to the formation of this molecule (Figure 1).<sup>15,16</sup>

In a more recent publication, they found some new derivatives of the cubic octamer when using higher concentrations of  $\text{SiO}_2$ .<sup>17</sup> This is the first point in the condensation sequence at which the proposed structures contain  $\text{Q}^4$  sites, the silicate building unit in the bulk material. Also, Harris et al. found a slightly varied cubic octamer exhibiting four  $\text{Q}^4$  sites at the corners, each with an additional  $\text{Si}(\text{OH})_3$  group connected to the cube.<sup>18</sup> Kinrade and Knight proposed that nucleating silicate solutions are composed of a limited number of small, highly condensed molecules in dynamic equilibrium and exclude the existence of embryonic precursor species with a specific structure.<sup>15,16,19</sup> Mintova et al. investigated the formation of different zeolite crystals from aqueous solutions using transmission electron microscopy (TEM), dynamic light scattering (DLS), and X-ray diffraction (XRD) and found direct conversion of amorphous gel particles, which were the first particles observed after the reaction start, to crystalline structures.<sup>20–22</sup> Also, Kragten et al. found subcolloidal nanoparticles during the clear-solution synthesis of silicalite-1 and suggested that the extracted particles are amorphous.<sup>23</sup> In contrast, Kirschhock et al. emphasized the idea of a distinctive molecule as a precursor in the synthesis of zeolites.<sup>24–27</sup> They used  $^{29}\text{Si}$  NMR spectroscopy to propose a silicate molecule of 36 silicon atoms with already implemented MFI topology to be the dominant precursor species in solution. Assembling these building blocks would lead to the formation

of zeolite crystals. However, this notion has been severely challenged by other groups.<sup>19,23,28</sup>

Despite the fact that mass spectrometry is one of the few techniques that is able to detect arrangements of several hundred atoms, which may allow them to come close to the crystallization point and approach it from the side of the solution, there are only two publications available that deal with mass spectrometry of prenucleating silicate solutions. In previous work, we proved the applicability of electrospray mass spectrometry (ESI MS) to investigate condensation reactions in alkaline silicate solutions.<sup>29</sup> Because the ionization process under ESI MS conditions is free of fragmentation reactions, it was possible to analyze many different silicate species simultaneously. We demonstrated the structure-directing effect of tetramethylammoniumhydroxide (TMAOH) and tetraethylammoniumhydroxide (TEAOH) on silicate formation, that is, in the former case, the formation of the cubic octamer,  $\text{Si}_8\text{O}_{20}\text{H}_7^-$ ,  $m/z$  551, and in the latter case, the formation of the prismatic hexamer,  $\text{Si}_6\text{O}_{15}\text{H}_5^-$ ,  $m/z$  413, as the final products. A second mass spectrometric investigation using H/D exchange processes in acidic silicate solutions has recently been published.<sup>30</sup> The authors tried to determine the number of hydrogen atoms in silicate species and, thus, tried to elucidate the structure of the species present. In addition to these studies using ESI MS, we had earlier introduced LILBID MS to study nucleating titanium and zirconium solutions.<sup>31</sup>

In the present work, we focused on aqueous solutions containing tetraalkylammoniumhydroxides (TAAOH) as the organic template and tetraalkoxysilanes (TAOS) as the silicate source. It was possible to carry out time-resolved measurements by using three different reactor systems: a tubular reactor, a syringe reactor, and a batch reactor, and we could follow the pathways of species development from smaller to larger silicate units. We show the influence of the length of the alkoxy group of the silanes on the hydrolysis rates, as well as the nature of the alkyl chain of the tetraalkylammoniumhydroxides on the condensation reaction of the silicates. Lowering the pH and increasing the reactant concentrations leads to conditions closer to precipitation of silica and is a first step for a more detailed study of the precipitation and crystallization of silica and silicates.

## Experimental Section

The silicate solutions were synthesized via clear-solution synthesis.<sup>32</sup> All reagents were obtained from commercial sources and used as received. As the silicate source, we used tetramethoxysilane (TMOS, 99%, Fluka, Steinheim, Germany), tetraethoxysilane (TEOS, 99%, Fluka, Steinheim, Germany), tetra-*n*-propoxysilane (TPOS, 97%, Lancaster, England), and tetra-*n*-butoxysilane (TBOS, 97%, Fluka, Steinheim, Germany). As the organic template, we used tetramethylammoniumhydroxide (TMAOH, 25% in water, purum, Fluka, Steinheim, Germany), tetraethylammoniumhydroxide (TEAOH, 35% in water, Aldrich, Steinheim, Germany), or tetra-*n*-propylammoniumhydroxide (TPAOH, 40% in water, Alfa Aesar). Methanol was purchased from

- (14) Harris, R. K.; Knight, C. T. G. *J. Chem. Soc., Faraday Trans. 2* **1983**, 79, 1539.  
 (15) Kinrade, S. D.; Knight, C. T. G.; Pole, D. L.; Syvitski, R. T. *Inorg. Chem.* **1998**, 37, 4272.  
 (16) Kinrade, S. D.; Knight, C. T. G.; Pole, D. L.; Syvitski, R. T. *Inorg. Chem.* **1998**, 37, 4278.  
 (17) Kinrade, S. D.; Donovan, J. C. H.; Schach, A. S.; Knight, C. T. G. *J. Chem. Soc., Dalton Trans.* **2002**, 1250.  
 (18) Harris, R. K.; Parkinson, J.; Samadi-Maybodi, A. *J. Chem. Soc., Dalton Trans.* **1997**, 2533.  
 (19) Knight, C. T. G.; Kinrade, S. D. *J. Phys. Chem. B* **2002**, 106, 3329.  
 (20) Mintova, S.; Olson, N. H.; Valchev, V.; Bein, T. *Science* **1999**, 283, 958.  
 (21) Mintova, S.; Olson, N. H.; Bein, T. *Angew. Chem., Int. Ed.* **1999**, 38, 3201.  
 (22) Mintova, S.; Petkov, N.; Karaghiosoff, K.; Bein, T. *Micropor. Mesopor. Mater.* **2001**, 50, 121.  
 (23) Kragten, D. D.; Fedeyko, J. M.; Sawant, K. R.; Rimer, J. D.; Vlachos, D. G.; Lobo, R. F.; Tsapatsis, M. *J. Phys. Chem. B* **2003**, 107, 10006.  
 (24) Kirschhock, C. E. A.; Ravishankar, R.; Verspeurt, F.; Grobet, P. J.; Jacobs, P. A.; Martens, J. A. *J. Phys. Chem. B* **1999**, 103, 4965.  
 (25) Kirschhock, C. E. A.; Ravishankar, R.; Van Looveren, L.; Jacobs, P. A.; Martens, J. A. *J. Phys. Chem. B* **1999**, 103, 4972.  
 (26) Ravishankar, R.; Kirschhock, C. E. A.; Knops-Gerrits, P.; Feijen, E. J. P.; Grobet, P. J.; Vanoppen, P.; De Schryver, F. C.; Miehe, G.; Fuess, H.; Schoeman, B. J.; Jacobs, P. A.; Martens, J. A. *J. Phys. Chem. B* **1999**, 103, 4960.  
 (27) Kirschhock, C. E. A.; Kremer, S. P. B.; Grobet, P. J.; Jacobs, P. A.; Martens, J. A. *J. Phys. Chem. B* **2002**, 106, 4897.

- (28) Ramanan, H.; Kokkoli, E.; Tsapatsis, M. *Angew. Chem., Int. Ed.* **2004**, 43, 4558.  
 (29) Bussian, P.; Sobott, F.; Brutschy, B.; Schrader, W.; Schüth, F. *Angew. Chem., Int. Ed.* **2000**, 39, 3901.  
 (30) Eggers, K.; Eichner, T.; Woenckhaus, J. *Int. J. Mass Spectrom.* **2005**, 244, 72.  
 (31) Sobott, F.; Schunk, S. A.; Schüth, F.; Brutschy, B. *Chem.—Eur. J.* **1998**, 4, 2353.  
 (32) Schoeman, B. J.; Sterte, J.; Otterstedt, J. E. *J. Chem. Soc. Chem. Commun.* **1993**, 994.

Merck KGaA, Darmstadt, Germany. Water was triply distilled. All samples were prepared in 30-mL polypropylene bottles equipped with magnetic stirrers.

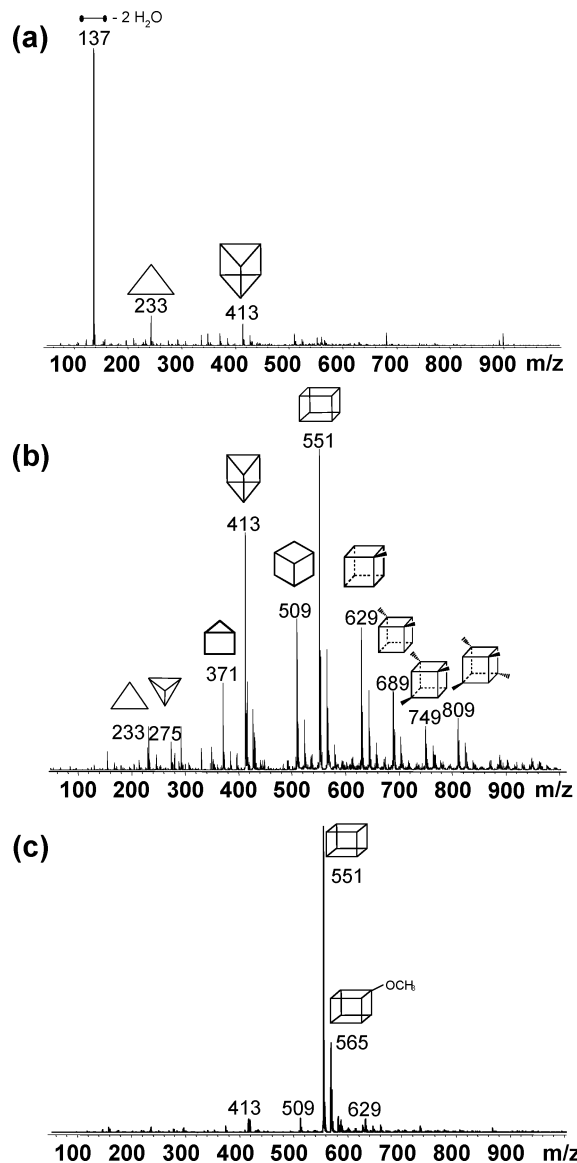
The general molar composition of the samples was  $\text{SiO}_2/\text{TAA}_2\text{O}/\text{H}_2\text{O}/\text{ROH} = 1.00:1.12:52.63:4.00$ . The samples were prepared by dissolving TAAOH (0.0038 mol) in the corresponding amount of water. The mixture was stirred for 5 min at 500 rpm, and tetraalkoxysilane (0.0034 mol) was added dropwise over 10 s while stirring was continued. For measuring the so-prepared samples, three different types of reactors were used depending on the time scales studied. For long reaction times, a batch reactor was employed. In the batch reactor experiment, the reagents were mixed as described, and small volumes of the sample were taken after defined reaction times and directly injected into the mass spectrometer using a syringe pump. This type of reactor enabled measurements from 5 min up to 24 h and longer. When using the syringe reactor, the mixed reagents were filled into a syringe, and the total volume of the syringe was measured within one run and continuously injected into the mass spectrometer, which enabled continuous measurements for up to 40 min in practice. The polymer tube reactor was used for short reaction times;<sup>33</sup> every experiment with a time scale below 4 min was performed using it. Here, the reagents were mixed directly in the tube reactor. The reactor was connected to a T-piece, which was fed by two syringes, one loaded with the tetraalkoxysilane, the other with a mixture of water/tetraalkylammonium-hydroxide. The flow in the tube was split by a second T-piece to adjust it to the requirements of the mass spectrometer. For all experiments, the flow rates into the mass spectrometer were set to  $100 \mu\text{L}/\text{h}$ .

The measurements were performed on a Bruker Esquire 3000 with an electronic ion trap or a Bruker Fourier Transform Ion Cyclotron Resonance mass spectrometer (FTICR MS) for high-resolution studies, both equipped with an ion source (Agilent) using an orthogonal sprayer alignment. The samples were measured with a capillary voltage of 4 kV, the cone-skimmer 1 voltage was  $-30.8 \text{ V}$ , and the cap exit offset was  $-71.6 \text{ V}$ . The desolvation temperature was set to  $250 \text{ }^\circ\text{C}$ . Mass calibration was performed using standards in the range from 100 to 3000 Da from Agilent.

## Results and Discussion

On adding TMOS to the aqueous solution containing TMAOH, it dissolves completely within seconds and no phase separation can be observed. The earliest spectrum was recorded two minutes after mixing the reactants. It shows one main signal at  $m/z$  137, which can be attributed to a dehydroxylated dimer,  $\text{Si}_2\text{O}_5\text{H}_1^-$  (Figure 2a).

Clearly, the hydrolysis of the silane is completely finished within two minutes and dimerization of the monomeric silicic acid,  $\text{Si}(\text{OH})_4$ , occurs. Both  $\text{Q}^1$  sites of the hydroxylated dimer,  $\text{Si}_2\text{O}_7\text{H}_5^-$ , seem to be quite instable in the gas phase of the mass spectrometer, because only a small signal at  $m/z$  173 is obtained for this anion. Dehydroxylation of two geminal OH groups leads to a dimer at  $m/z$  155, whose mass is reduced by the mass of one water molecule compared to the  $m/z$  173 signal; a second dehydroxylation step results in the predominant species at  $m/z$  137. This kind of water elimination leads to a  $\text{Si}=\text{O}$  double bond, which is only stable in the gas phase of the mass spectrometer and only occurs at  $\text{Q}^0$ ,  $\text{Q}^1$ , and  $\text{Q}^2$  sites in decreasing proportions. In contrast, water-loss effects can be excluded at  $\text{Q}^3$  and  $\text{Q}^4$  sites. With increasing reaction time, a multitude of silicate structures is formed; the more dominant species are additionally singly or doubly methoxylated, which is indicated by satellite peaks at  $+m/z$  14 and  $+m/z$  28,



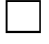

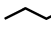

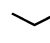


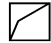





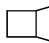







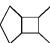


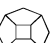







**Figure 2.** ESI negative mass spectra of the system TMOS–TMAOH– $\text{H}_2\text{O}$  recorded after different reaction times: (a) 2 min, (b) 30 min, (c) 24 h after the start of the reaction. Each line in the stick figures represents a  $\equiv\text{Si}-\text{O}-\text{Si}\equiv$  siloxane linkage. The spectrum after 2 min was recorded using the tube reactor, the two others using the batch reactor.

respectively (Figure 2b). It has turned out that the detected alkoxylation is partially caused by alcohol in solution resulting from the hydrolysis of the alkoxy silane as well as by gas-phase reactions within the mass spectrometer, which we will discuss in more detail in a forthcoming publication. Up to a mass of about  $m/z$  450, smaller oligomers up to the hexamer at  $m/z$  431 are detected. In accordance with Kinrade and Knight, the suggested structures show the tendency of the silicate anions to be as condensed as possible.<sup>19</sup> Thus, closed-ring systems are formed and open-chain structures are avoided. From  $m/z$  400, the species grow larger, continuing this tendency by forming 3-dimensional cage structures. Within these, one can identify basically symmetric molecules, such as the double 3 ring (D3R) and the double 4 ring (D4R), resembling the structure of the prismatic hexamer and the cubic octamer, respectively, as well as derivatives of the latter. Possible suggestions for the molecular structures of these derivatives, which are detected above  $m/z$  629,

(33) Linden, M.; Schunk, S. A.; Schüth, F. *Angew. Chem., Int. Ed.* **1998**, *37*, 821.

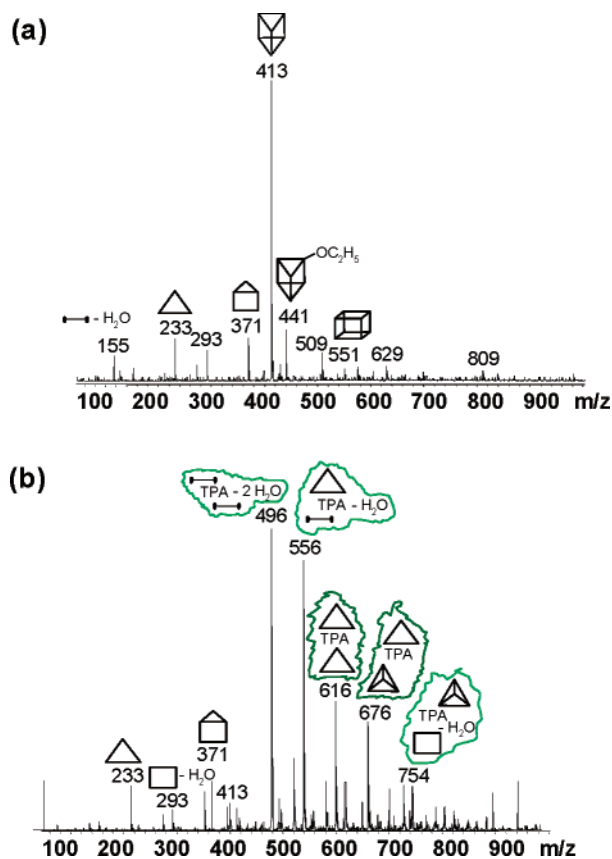
**Table 1.** Accurate Determined  $m/z$  Values Observed in the System TMOS-TMAOH-H<sub>2</sub>O Using FTICR MS. The Corresponding Sum Formulas Cannot Be Unambiguously Assigned to One Possible Structure; Therefore, Several Structures Are Listed

Observed Mass Da	Calculated Mass / Da	Deviation Da	Sum Formula	Possible Structures
76,96750	76,97005	-0,00255	Si <sub>1</sub> O <sub>3</sub> H <sub>1</sub> <sup>-</sup>	▪ -1 H <sub>2</sub> O
94,97748	94,98061	-0,00313	Si <sub>1</sub> O <sub>4</sub> H <sub>3</sub> <sup>-</sup>	▪
136,92956	136,93680	-0,00724	Si <sub>2</sub> O <sub>5</sub> H <sub>1</sub> <sup>-</sup>	— -2 H <sub>2</sub> O
172,95108	172,95794	-0,00686	Si <sub>2</sub> O <sub>7</sub> H <sub>5</sub> <sup>-</sup>	—
232,92037	232,92469	-0,00433	Si <sub>3</sub> O <sub>9</sub> H <sub>5</sub> <sup>-</sup>	 -1 H <sub>2</sub> O
274,87821	274,88088	-0,00267	Si <sub>4</sub> O <sub>10</sub> H <sub>3</sub> <sup>-</sup>	 -3 H <sub>2</sub> O
292,88967	292,89145	-0,00178	Si <sub>4</sub> O <sub>11</sub> H <sub>5</sub> <sup>-</sup>	 -1 H <sub>2</sub> O,  -1 H <sub>2</sub> O,  -2 H <sub>2</sub> O
352,86069	352,85821	0,00248	Si <sub>5</sub> O <sub>13</sub> H <sub>5</sub> <sup>-</sup>	 -1 H <sub>2</sub> O,  -3 H <sub>2</sub> O
370,87068	370,86877	0,00190	Si <sub>5</sub> O <sub>14</sub> H <sub>7</sub> <sup>-</sup>	 -1 H <sub>2</sub> O,  -1 H <sub>2</sub> O, 
412,82492	412,82496	-0,00004	Si <sub>6</sub> O <sub>15</sub> H <sub>5</sub> <sup>-</sup>	
430,83566	430,83553	0,00013	Si <sub>6</sub> O <sub>16</sub> H <sub>7</sub> <sup>-</sup>	 -1 H <sub>2</sub> O,  -1 H <sub>2</sub> O, 
508,81241	508,81286	-0,00044	Si <sub>7</sub> O <sub>19</sub> H <sub>9</sub> <sup>-</sup>	 -1 H <sub>2</sub> O, 
550,76780	550,76905	-0,00125	Si <sub>8</sub> O <sub>20</sub> H <sub>7</sub> <sup>-</sup>	
628,74570	628,74637	-0,00067	Si <sub>9</sub> O <sub>23</sub> H <sub>9</sub> <sup>-</sup>	 -1 H <sub>2</sub> O,  -1 H <sub>2</sub> O, 
688,71289	688,71313	-0,00023	Si <sub>10</sub> O <sub>25</sub> H <sub>9</sub> <sup>-</sup>	 -1 H <sub>2</sub> O, 
748,67817	748,67988	-0,00171	Si <sub>11</sub> O <sub>27</sub> H <sub>9</sub> <sup>-</sup>	 -2 H <sub>2</sub> O,  -3 H <sub>2</sub> O,  -1 H <sub>2</sub> O
808,64383	808,64664	-0,00281	Si <sub>12</sub> O <sub>29</sub> H <sub>9</sub> <sup>-</sup>	 -3 H <sub>2</sub> O,  -3 H <sub>2</sub> O
868,61275	868,61340	-0,00065	Si <sub>13</sub> O <sub>31</sub> H <sub>9</sub> <sup>-</sup>	 -4 H <sub>2</sub> O,  -4 H <sub>2</sub> O
928,57994	928,58015	-0,00022	Si <sub>14</sub> O <sub>33</sub> H <sub>9</sub> <sup>-</sup>	 -5 H <sub>2</sub> O
1.084,52670	1.084,53480	-0,00810	Si <sub>16</sub> O <sub>39</sub> H <sub>13</sub> <sup>-</sup>	 -5 H <sub>2</sub> O, 

have the cubic octamer as the basic structure and are enlarged gradually by condensing silicate monomer units to the corners of the cube. For the first time during the condensation sequence, these species exhibit Q<sup>4</sup> sites, the silicate building unit in the bulk material, and these have already been characterized by <sup>29</sup>Si NMR spectroscopy.<sup>17</sup> The silicates formed in this way are detectable up to a mass of the pentadecamer with 7 monomer units added to the cube at  $m/z$  989. The condensation between two cubic octamers, first found in samples with an increased SiO<sub>2</sub> content,<sup>18</sup> results in a hexadecamer anion, which, however, only could be detected at a low intensity (Table 1). At the end of the condensation reaction, the intermediate silicate species disappear and contribute to the formation of the predominant species at  $m/z$  551, in accordance with many observations that attribute the formation of the cubic octamer to the presence of TMA<sup>+</sup> (Figure 2c).<sup>12,15,16,17,29,34–37</sup>

As already pointed out, the use of different ammonium salts as the organic template leads to different products.<sup>35,36</sup> In the presence of TMA<sup>+</sup>, the formation of D4R is favored (Figure 2c), whereas in TEA<sup>+</sup>-containing samples, the equilibrium is pushed to the side of D3R (Figure 3a). In spectra of TPA<sup>+</sup>-containing samples, signals are surprisingly observed, which can be attributed to silicate-TPA<sup>+</sup> clusters and also signals of smaller silicates (Figure 3b). Clearly, in the given concentration range, the affinity of TPA<sup>+</sup> to coordinate anions is strong enough to keep smaller silicates in the direct environment of TPA<sup>+</sup> and to prevent them from growing larger. However, clustering of compounds is nothing unusual under ESI MS conditions and can be influenced by instrumental parameters. We could not find such an influence on the extent of clustering when varying

(34) McCormick, A. V.; Bell, A. T. *Catal. Rev.-Sci. Eng.* **1989**, *31*, 97.(35) Hendricks, W. M.; Bell, A. T.; Radke, C. J. *J. Phys. Chem.* **1991**, *95*, 9513.(36) Hendricks, W. M.; Bell, A. T.; Radke, C. J. *J. Phys. Chem.* **1991**, *95*, 9519.



**Figure 3.** Different ammonium salts lead to different product distributions: (a) in TEA<sup>+</sup>-containing samples, the formation of D3R is favored, (b) TPA<sup>+</sup> promotes the formation of clusters between smaller silicates and TPA<sup>+</sup> cations. Both spectra were recorded after 24 hours using the batch reactor.

the cap exit voltage, but we cannot exclude that a part of it may be generated in the gas phase of the mass spectrometer. Nevertheless, applying the same experimental conditions on TMA<sup>+</sup>- and TEA<sup>+</sup>-containing samples reveals no clustering at all.

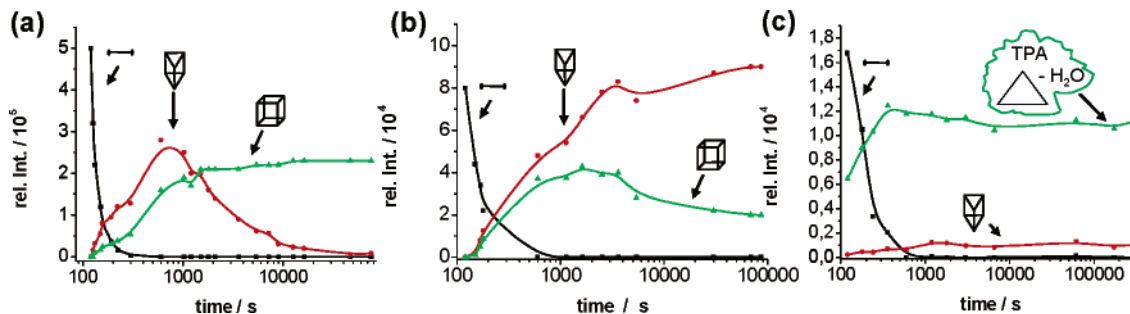
Other authors have already pointed out the special role of TPA<sup>+</sup> on the condensation of silicates in zeolite synthesis reactions.<sup>24,38–41</sup> The favored formation of open or half-open structures in the presence of TPA<sup>+</sup> is commonly seen as a requirement in the synthesis of zeolites. Burkett and Davis formulated a mechanism where water species around TPA<sup>+</sup> molecules would be sequentially replaced by silicate units, which leads to a preorganization of the silicates due to the rather hydrophobic character of the TPA<sup>+</sup>.<sup>39–41</sup> The observation of clusters in our studies supports these notions. In our investiga-

tion, no larger units than hexamers were detected as parts of the clusters. The occurrence of only small silicates with mainly Q<sup>2</sup> sites can be attributed to the fact that—in contrast to solutions leading to zeolite formation—the concentration of silicates is not high enough to form larger structures and that the solutions were not heated.

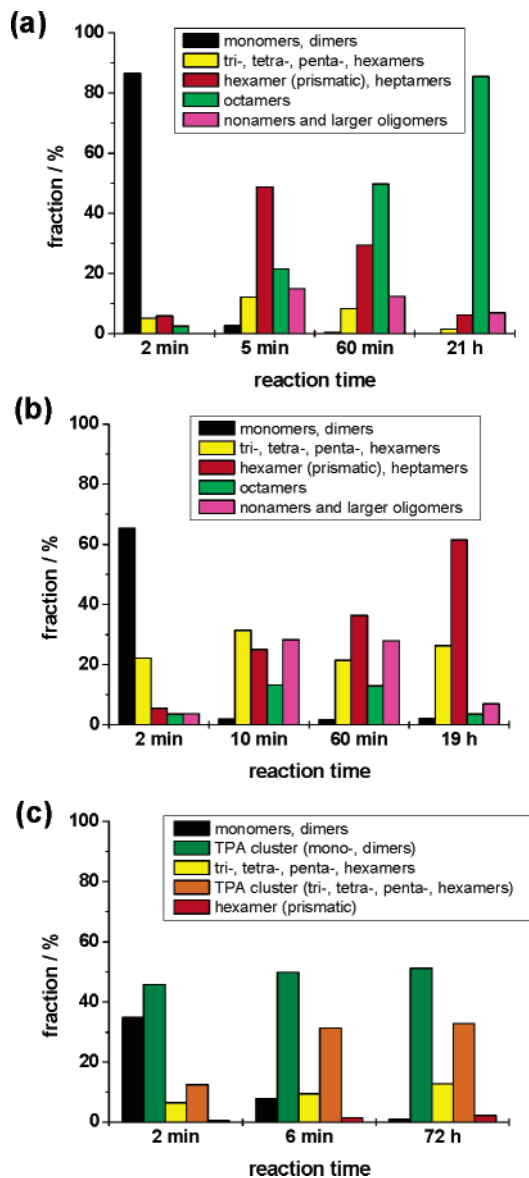
Figure 4 shows the relative intensities over time of some silicate species occurring in TMA<sup>+</sup>-, TEA<sup>+</sup>-, and TPA<sup>+</sup>-containing samples. At the end of every chart, the main product can clearly be identified. In TMA<sup>+</sup>-containing samples, the hexamer plays the role of an intermediate, which disappears after some time. TEA<sup>+</sup> promotes the formation of the prismatic hexamer, whereas the intensity of the cubic octamer decreases. In the presence of TPA<sup>+</sup> cations, the above-mentioned silicate–TPA<sup>+</sup> clusters are formed after a short time. Cage structures are only detectable in a minor amount.

The overall product distribution in these samples at certain reaction times is illustrated in Figure 5. Silicate species showing a similar temporal evolution are clustered. The most narrow distribution can be found in TMA<sup>+</sup>-containing samples: more than 85% of all silicates exist in the form of the cubic octamer and its alkoxyated derivatives. In TEA<sup>+</sup>-containing samples, only around 60% of all silicates are present in the form of the prismatic hexamer and the heptamer. If TPA<sup>+</sup> is present, approximately 80% of the silicate species are coordinated by one TPA<sup>+</sup> cation, whereas the fraction of free oligomers is less than 15%. Obviously, the cyclic silicates, i.e., trimers, tetramers, pentamers, and hexamers, are less effectively coordinated in comparison to the linear ones, i.e., monomers and dimers: 72 h after the start of the reaction, one can detect a fraction of free cyclic silicates of about 13%; in contrast the fraction of free monomers and dimers is below 1%.

The length of the alkoxy chain of the tetraalkoxysilane and its influence on the hydrolysis and condensation steps of the silicates was also investigated using tetramethoxy-, tetraethoxy-, tetra-*n*-propoxy-, and tetra-*n*-butoxysilane as silica precursors. We observed that the kind of alkoxy group basically influences the rate of the hydrolysis of the silane. The larger the alkoxy group, the slower is the hydrolysis of the silane. This is in agreement with literature data obtained by various researchers.<sup>42–45</sup> Figure 6 shows the evolution of silicate species in samples that contain TMOS, TEOS, or TPOS as the silicate source. In addition to the hexamer and the octamer, the product of the first hydrolysis step, Si(O)(OR)<sub>3</sub><sup>−</sup>, is shown in every chart except for the TMOS-containing sample, where no methoxylated monomeric units could be detected. In all samples, TMAOH was used as the ammonium salt, so that at the end of every

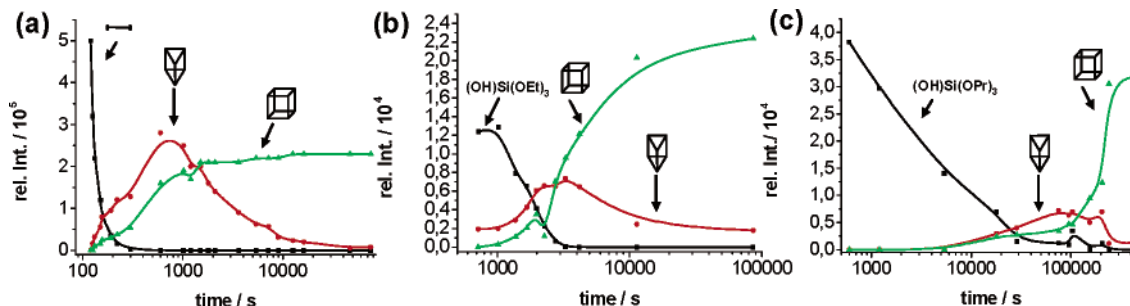


**Figure 4.** Relative intensities over the time of some silicate species in measurements varying the ammonium salt. The samples contain (a) TMA<sup>+</sup>, (b) TEA<sup>+</sup>, (c) TPA<sup>+</sup>, each with TMOS.



**Figure 5.** Silicate distribution in (a) TMA<sup>+</sup>, (b) TEA<sup>+</sup>, and (c) TPA<sup>+</sup> containing samples as a function of reaction time. Only in a TPA<sup>+</sup> environment are clusters formed consisting of TPA<sup>+</sup> cations and smaller silicates, whereas no larger silicates than the hexamer are detected.

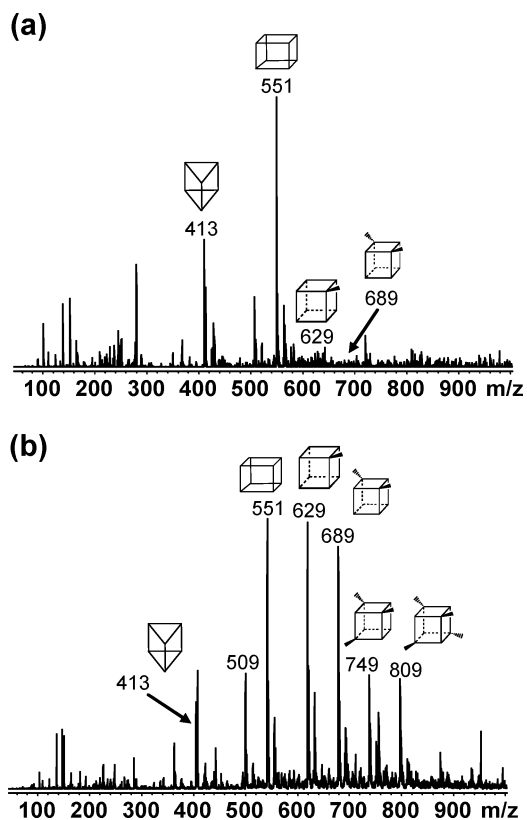
reaction, the product distribution is the same. The hydrolysis of TMOS is completed within less than two minutes, because even in the first recorded spectrum (two minutes after the reaction start), there is no evidence for species such as Si(O)(OCH<sub>3</sub>)<sub>3</sub><sup>-</sup>, Si(OH)(O)(OCH<sub>3</sub>)<sub>2</sub><sup>-</sup>, or Si(OH)<sub>2</sub>(O)(OCH<sub>3</sub>)<sup>-</sup>. In the case of TEOS, a phase separation between the aqueous



**Figure 6.** Relative intensities over the time of some silicate species in measurements varying the alkoxy silane. The samples contain (a) TMOS, (b) TEOS, (c) TPOS, each with TMA<sup>+</sup>.

phase and the silane phase can be observed for up to 1 h after mixing the reactants, whereas in the case of TPOS, it takes even up to 2 days for a one-phase system to form. When using TBOS, partial hydrolysis can be shown only after two weeks at increased temperature.

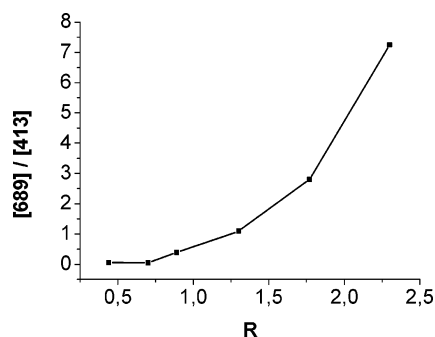
In another series of measurements, we investigated the influence of the ratio of TMOS to TMAOH on the tendency of silicate species to condensate. The amount and the composition of the solvent remained unchanged. Figure 7 shows two mass



**Figure 7.** Two spectra of samples with a varying ratio of TMOS to TMAOH after 24 h using the batch reactor; the  $R$  value is (a)  $R = 0.4$ , (b)  $R = 1.8$  with  $R = [\text{TMOS}]/[\text{TMAOH}]$ . Increase of the concentration of TMOS leads to a shift in the product distribution to heavier masses.

spectra of samples with  $R = 0.4$  and  $R = 1.8$  with  $R = [\text{TMOS}]/[\text{TMAOH}]$ .

A shift of the product distribution from lighter masses to heavier masses is observed with an increasing amount of TMOS. At  $R$  values smaller than 1, the formation of smaller silicate structures is enhanced, the cubic octamer always being the main product. A further increase of the  $R$  value up to 2.3 leads to heavier species up to  $m/z$  869. Figure 8 demonstrates the shift



**Figure 8.** Ratio of the relative intensities of the species at  $m/z$  689 to  $m/z$  413 in dependency of the  $R$  value.

in the product distribution from smaller silicate structures to larger units taking the hexamer and the decamer as an example.

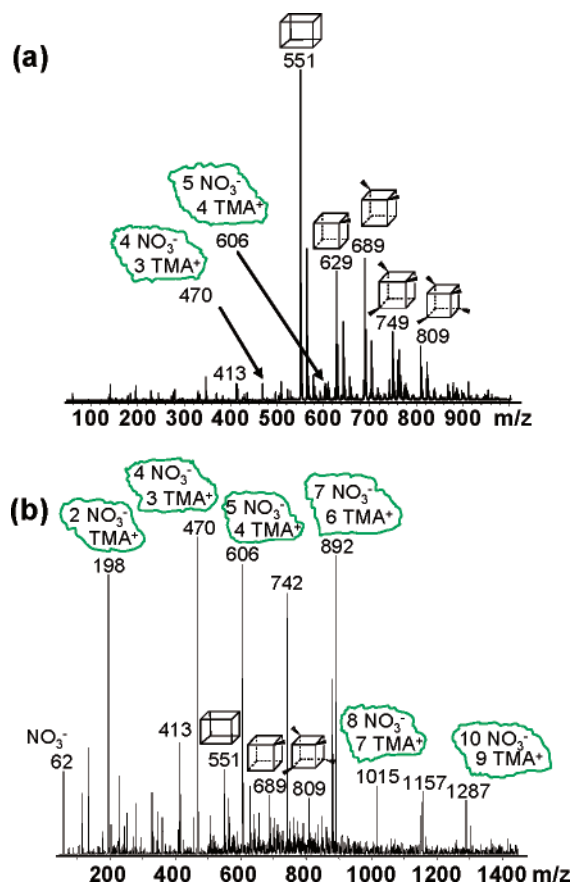
In samples with a  $R$  value below 1, there is only a very small amount of the decamer detectable, whereas an  $R$  value above 1.3 results in higher intensities for the decamer than for the hexamer. A tremendously accelerated reaction with an increasing amount of TMOS is observed. At a ratio of  $R = 1.8$ , the condensation reactions are almost completely finished after 10 min. In the next 3 h, the spectra remain nearly unchanged.

It is known that silicates are soluble at high pH values and that they precipitate when lowering the pH. We approached the precipitation point from the side of the solution by decreasing the pH value from 14 to 12 using nitric acid. Below a pH of 12,  $\text{SiO}_2$  precipitated from solution, preventing further mass spectrometric investigations. Figure 9a shows a spectrum of the system TMOS/TMAOH/ $\text{H}_2\text{O}$  at a pH of 12.4 after 24 hours.

A shift of the product distribution from lighter to heavier masses at decreased pH values can be observed, as found in the former experiment when varying the  $R$  value. The rate of the reactions is also increased. The main condensation steps appear to be completely finished 3 min after the start of the reaction. Up to this point, also the formation of  $\text{TMA}^+ - \text{NO}_3^-$  clusters is detected, resulting in  $m/z$  values up to  $m/z$  1,500 (Figure 9b). With the occurrence of larger silicate species these clusters disappear again. Obviously, the  $\text{TMA}^+$  cations are now mainly involved in the coordination of silicate structures. Only low intensities of  $\text{TMA}^+ - \text{NO}_3^-$  clusters at  $m/z$  470 and  $m/z$  606 are observed, consisting of 3  $\text{TMA}^+$  and 4  $\text{NO}_3^-$  ions and 4  $\text{TMA}^+$  and 5  $\text{NO}_3^-$  ions, respectively.

### Summary and Conclusions

We have shown that ESI MS is a powerful method to obtain detailed insight in the processes occurring in silicate solutions. With the help of adapted reactors, time-resolved experiments become possible, which allows to follow the development of different silicate solution species also in dependence on the presence of other additives, such as different alkylammonium ions. This methodology nicely complements the powerful NMR



**Figure 9.** Increase in the tendency of condensation of silicates by lowering the pH: (a) 24 h after the reaction start at pH 12.4, an increased amount of larger units is detected; (b) 3 min after the reaction start,  $\text{TMA}^+ - \text{NO}_3^-$  clusters are formed, which disappear again after 10 min and are detectable only at low intensities after 24 h. Both spectra were recorded using batch reactors.

tools for the analysis of silicate speciation, in that the achievable time resolution is higher, however, at the expense of quantitative information and structural identification—which is, however, certainly not trivial by NMR techniques as well. As opposed to NMR spectroscopy, the mass spectrometric techniques have the advantage that they are in principle suitable for the analysis also of other systems and thus rather generic, whereas not all types of atoms can be studied with NMR techniques.

The present studies were carried out at silicate concentrations that are too low for zeolite formation. However, the results reported have direct implications also for zeolite synthesis and clearly point the way for studies at higher silicate concentrations. Especially interesting is the fact that the  $\text{TPA}^+$  ion has a high ability for silicate coordination, so that  $\text{TPA}^+ - \text{silicate}$  clusters can be detected in the gas phase, as opposed to alkylammonium ions with shorter alkyl chains. This underlines the special role the  $\text{TPA}^+$  ion has as a template in zeolite synthesis. Although the smaller tetraalkylammonium ions are still rather hydrophilic, the  $\text{TPA}^+$  is sufficiently hydrophobic to organize silicate species around itself, thus probably inducing the formation of the MFI structure, the structure of the most often investigated high silica zeolites, ZSM-5 and silicalite-1.

At lower pH values, condensation proceeds toward higher oligomers in solution, which is in agreement with expectations. However, even close to the precipitation point, no silicate clusters corresponding to one of the sizes reported by Kirschhock

- (37) Groenen, E. J. J.; Kortbeek, A. G. T. C.; Mackay, M.; Sudmeijer, O. *Zeolites* **1986**, *6*, 403.  
 (38) Schoeman, B. J.; Regev, O. *Zeolites* **1996**, *17*, 447.  
 (39) Burkett, S. L.; Davis, M. E. *J. Phys. Chem.* **1994**, *98*, 4647.  
 (40) Burkett, S. L.; Davis, M. E. *Chem. Mater.* **1995**, *7*, 920.  
 (41) Burkett, S. L.; Davis, M. E. *Chem. Mater.* **1995**, *7*, 1453.  
 (42) Iler, R. K. *The Chemistry of Silica*; Wiley: New York, 1979.  
 (43) Brinker, C. J.; Scherer, G. W. *Sol-Gel Science*; Academic Press: Boston, 1990.  
 (44) Schmidt, H.; Scholze, H.; Kaiser, A. *J. Non-Cryst. Solids* **1984**, *63*, 1.  
 (45) Bernards, T. N. M.; van Bommel M. J.; Boonstra, A. H. *J. Non-Cryst. Solids* **1991**, *134*, 1.

et al.<sup>5,24,25</sup> have been detected in our experiments. It has to be taken into account, though, that in contrast to these studies, our investigations were carried out at lower concentrations, which could lead to different speciation in solution. Work is under way to extend our investigations to conditions identical to those used in the zeolite nucleation studies used by Kirschhock and

others, to help to solve the puzzle of zeolite nucleation from clear solutions.

**Acknowledgment.** Partial financial support by the Leibniz program of the DFG is gratefully acknowledged.

JA057423R